PORE SCALE SIMULATION OF MAGNETOSOLUTAL MICROCONVECTION IN FERROFLUID SATURATED POROUS STRUCTURES

D. Zablotsky[1], E. Blums[1]
Affiliation: [1]Institute of Physics of University of Latvia, 32 Miera iela, Salaspils, LV-2169, Latvia
e-mail address of corresponding author: dmitrijs.zablockis@gmail.com

Abstract: We consider an idealized model of ferrofluid saturated porous medium composed of microscale non-magnetic inclusions with simple geometry. The application of homogeneous magnetic field induces complicated pattern of internal demagnetizing fields owing to the difference in magnetic permeability. In turn, the imbalance of ferroparticle concentration is created by non-uniform heating and associated colloidal thermophoresis. Numerical simulations of magnetosolutal microconvection show significant intensification of pore-scale mixing and appearance of solvent flux in the direction of temperature gradient.

1. Introduction

Ferrofluids – colloidal solutions of magnetic nanoparticles – exhibit pronounced Soret effect, i.e. colloidal thermophoresis. The influence of magnetic field on the drift of colloidal particles attracts interest as a means of control and intensification of mass transport in these media. While theory predicts that in bulk solutions the direct dependence of molecular mass transport coefficients on homogeneous magnetic field is weak [1]-[3], specific microconvective phenomena, i.e. magnetic solutal microconvection, may appear [4]-[5] causing significant intensification of mass transfer. Recent experimental evidence [6]-[7] suggests that magnetic phenomena are also quite significant in porous environments or membranes resulting in considerable attenuation of the thermophoretic separation due to enhanced mixing. It is hypothesized that similar magnetic microconvection may be partially responsible for this effect [8].

When magnetic field is applied to a ferrofluid saturated porous medium the jump of magnetic permeability across the boundary of non-magnetic inclusions may cause the appearance of significant gradients of internal magnetic field in the vicinity of the interface. A system of such inclusions thus forms markedly nonhomogeneous internal magnetic field within the porous environment. In turn, in the conditions of non-uniform heating the strong colloidal thermophoresis induces the formation of corresponding gradients of ferroparticle concentration. Both the appearance of the spatial non-homogeneity of the distribution of dispersed magnetic phase and the internal magnetic field contribute to the formation of the associated non-potential magnetosolutal buoyant force, which may entrain the ferrofluid and create pore-scale magnetosolutal microconvection. Apart from pore-scale microconvective circulations [8]-[9], the formation of integral flow is possible in the vicinity of the inclusions [8].

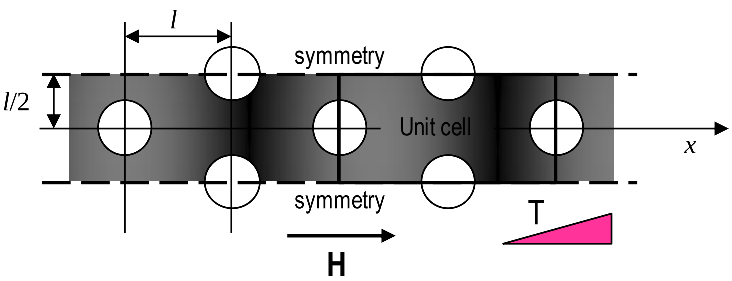

Figure 1: Scheme of the arrangement – non-magnetic cylindrical elements immersed in ferrofluid, temperature gradient and magnetic field are applied across the porous structure

Here we report preliminary results of numerical simulations of pore-scale magnetosolutal microconvection in geometrically simple model of porous media. We create a 1D arrangement of non-magnetic microscale cylinders immersed in ferrofluid (Fig.1). The porosity of the system is $\varepsilon=1-\pi/l^2$. A temperature gradient is applied across the structure and homogeneous external magnetic field is imposed in the same direction.

2. Magnetic microconvection

The magnetic force density acting on ferrofluid due to magnetic field is expressed by Kelvin body force term $\mathbf{F}=\mu_0(\mathbf{M}\nabla)\mathbf{H}$ with **M** – magnetization of ferrofluid and **H** – magnetic field. Assuming $\mathbf{M}=\chi(c,H)\mathbf{H}$, where $\chi(c,H)$ – magnetic susceptibility at given mass concentration and magnetic field, and with linear relationship for the magnetic susceptibility $\chi(c,H)=\chi_0(1+\chi_c\Delta c)$, where $\Delta c=c-c_0$, c_0 – reference mass concentration, $\chi_c=1/c_0$ and χ_0 – susceptibility at reference parameters, the non-potential part of the force density becomes $\mathbf{F}=\mu_0\chi_0\chi_c\Delta cH_0\nabla[(\mathbf{h}+\mathbf{\Delta H}/2H_0)\mathbf{\Delta H}]$ with $\mathbf{\Delta H}=\mathbf{H}-\mathbf{H_0}$, $\mathbf{H_0}=H_0\mathbf{h}$ – reference magnetic field, **h** – unit vector. Thus variation of ferroparticle concentration and magnetic field can produce magnetic convection in ferrocolloid.

The diffusive dynamics of colloidal nanoparticles is very slow and are only relevant on submillimetre lengthscales. In turn, the Schmidt number $Sc=\eta(\rho D)^{-1}$, where η and ρ – viscosity and density of ferrocolloid, D – diffusivity of ferroparticles, expresses the ratio of momentum and mass diffusivities and is of the order 10^4-10^5. The magnetosolutal microconvection then is creeping convection. Introducing characteristic scales for length L, time L^2D^{-1}, magnetic field $\overline{\Delta H}$, concentration perturbation $\overline{\Delta c}$ the dynamics of the ferrocolloid is described by dimensionless Stokes equation

$$-\nabla p+\Delta\mathbf{u}+Rm_c c\nabla[(\mathbf{h}+r_H\boldsymbol{\delta}\mathbf{H})\boldsymbol{\delta}\mathbf{H}]=0 \tag{1}$$

and the continuity condition $\nabla\cdot\mathbf{u}=0$. Here $r_H=\overline{\Delta H}/2H_0$ typically does not exceed 5% and is disregarded. The magnetosolutal Rayleigh number is $Rm_c=\mu_0\chi_0\chi_c H_0 L^2(\eta D)^{-1}\overline{\Delta c}\,\overline{\Delta H}$.

In non-isothermal ferrocolloid the linearized mass flux due to diffusion and thermophoresis is $\mathbf{J}=\mathbf{u}c-D\nabla c-c_0(1-c_0)DS_T\nabla T$ [10], where S_T is Soret coefficient. For now we neglect magnetophoretic contributions. Introducing the thermal scale $\overline{\Delta c}=c_0(1-c_0)|S_T|\overline{\Delta T}$ the normalized concentration dynamics equation

$$\frac{\partial}{\partial t}c+\mathbf{u}\nabla c=\Delta(c-T) \tag{2}$$

The Lewis number $Le=\alpha D^{-1}$ characterizing the ratio of thermal and mass diffusivities is also very large in ferrofluids. Thus, the temperature dynamics is much faster than that of concentration and magnetosolutal microconvection does not influence the distribution of temperature. We impose the temperature gradient gradT and calculate $\overline{\Delta T}=\mathrm{gradT}\cdot L$.

A non-magnetic cylinder immersed in ferrofluid with magnetic permeability $\mu_0=1+\chi_0$ and placed in homogeneous magnetic field creates around itself magnetic perturbation $\boldsymbol{\delta}\mathbf{H}$. In dimensionless form (the radius of the cylinder is assumed as length scale L)

$$\boldsymbol{\delta}\mathbf{H}=\mathrm{sign}(K_H)\frac{\cos(\Theta)}{r^2}\mathbf{e_r}+\mathrm{sign}(K_H)\frac{\sin(\Theta)}{r^2}\mathbf{e}_\Theta \tag{3}$$

where r and Θ, $\mathbf{e_r}$ and $\mathbf{e}_\Theta$ – cylindrical coordinates and basis vectors, $K_H=\dfrac{1-\mu_0}{1+\mu_0}$,

$\overline{\Delta H} = |K_H| H_0$. We calculate magnetic perturbation produced by an array of non-magnetic cylinders directly from Maxwell's equations, but the result corresponds to a superposition of 2D dipoles (3).

For typical ferrofluid parameters (S_T=0.1K^{-1}, η=0.001Pa s, D=2·10^{-11}m s^{-2}, c_0=0.15, particle diameter 8 nm, particle spontaneous magnetization 5·10^5 A m^{-1}), external field 0.1T and imposed temperature gradient corresponding to a temperature difference of 20K applied across a 1mm thick porous membrane the magnetosolutal Rayleigh number in the vicinity of cylindrical inclusion with radius 2μm reaches Rm_c=50. This is enough to cause significant microconvective particle transfer and we use this value in simulations.

3. Results

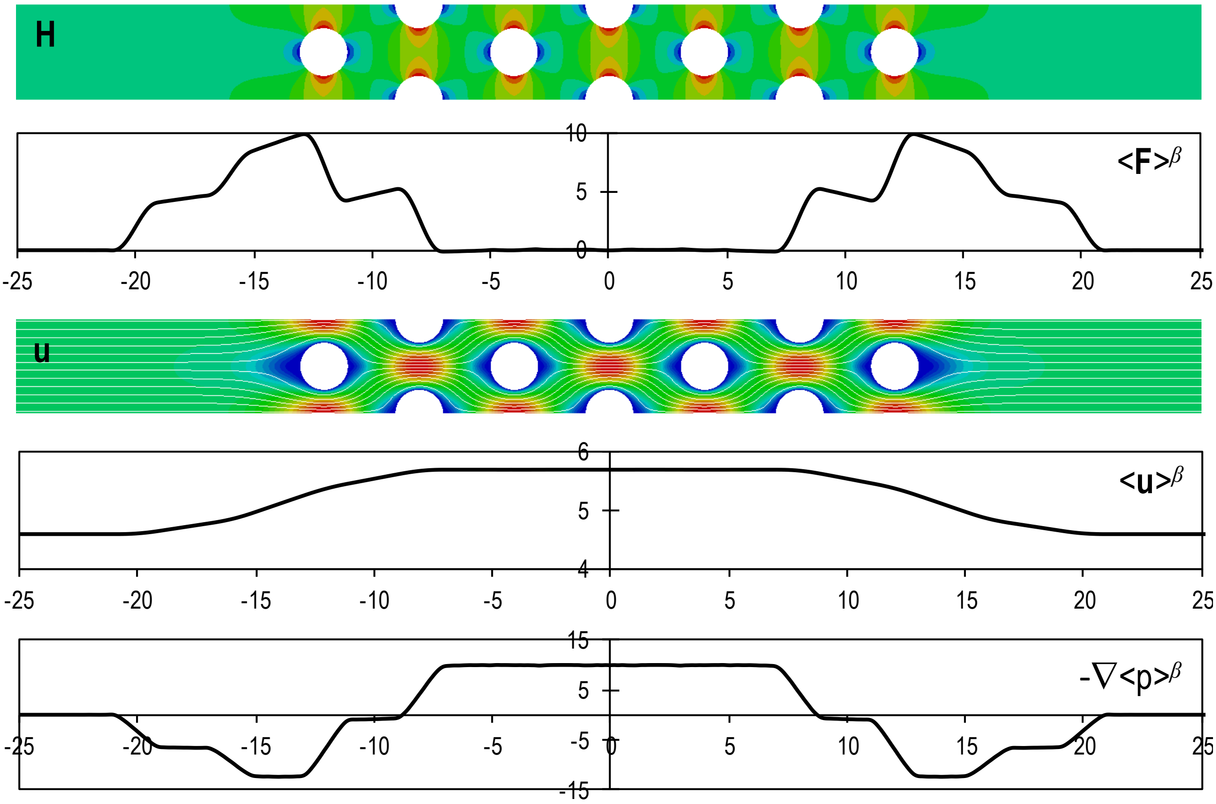

Figure 2: Case 1 simulation (ε=0.8, fixed concentration gradient), from top to bottom – perturbation of magnetic field H, plot of averaged magnetic force <**F**>$^\beta$, streamlines of velocity **u**, plot of averaged velocity <**u**>$^\beta$, plot of the gradient of averaged pressure -∇<p>$^\beta$

We start from initial concentration distribution c=-x, which corresponds to a stationary stratification created by temperature T=x. We have performed two series of simulations: in the first case we solve only the Stokes equation and the initial concentration distribution is not allowed to change (case 1). As expected, the calculated distribution of magnetic field perturbation H=**h·δH** is highly inhomogeneous (Fig.2) and so is the magnetic force $\mathbf{F} = Rm_c c \nabla H$. In order to reveal the macroscopic structure of the magnetic forces we perform spatial averaging. The correct average in periodic porous structures is the cellular average across a unit cell [11]. Interestingly, the averaged magnetic force density <**F**>$^\beta$ vanishes in the bulk of the porous structure and only remains in the immediate vicinity of the membrane surface, reaching sharp maximum within approximately a single period of the porous structure at both ends of the membrane. While the averaged magnetic force is well localized, its maximum value is proportional to the value of concentration at both ends of the membrane.

So, when a concentration gradient is applied across the porous membrane, the total magnetic force is proportional to the thickness of the membrane.

In the second series of calculations we solve also the concentration equation, advancing to the stationary/quasistationary state (case 2). In this case, the averaged concentration gradient decreases within the porous membrane (Fig.3) due to the change of porosity. In turn, the distribution of the averaged magnetic force becomes asymmetric with respect to the midpoint of the membrane. A component of the averaged magnetic force appears within the bulk of the membrane counteracting the pressure difference created by the forces in the vicinity of the membrane surface. These are the consequences of convective dispersion of concentration within the porous membrane. It can be expected that in 2D membranes these effects may lead to instabilities and oscillations.

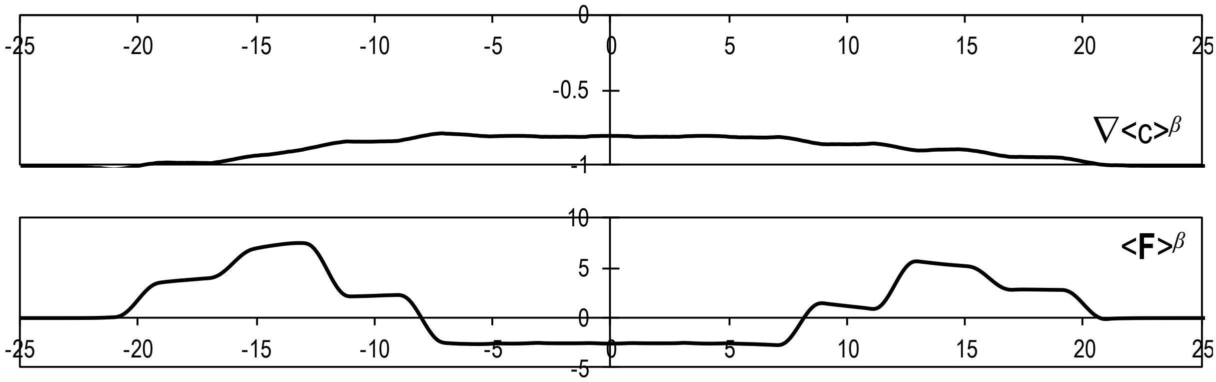

Figure 3: Case 2 simulations (ε=0.8, concentration can change), from top to bottom – plot of the gradient of averaged pressure -∇<p>$^{\beta}$, plot of averaged magnetic force <**F**>$^{\beta}$.

In the framework of Darcy theory the relationship between the averaged quantities should hold in the bulk of the porous membrane [11]

$$\langle \mathbf{u} \rangle^{\beta} = -\frac{K}{\varepsilon} \nabla \langle p \rangle^{\beta} \tag{4}$$

where K is the permeability tensor, which we calculate by solving the closure problem numerically for a unit cell [11]. In the series of calculations when the concentration gradient is fixed (case 1) the averaged magnetic force <**F**>$^{\beta}$ vanishes within the porous structure. That is why it is absent from (4).

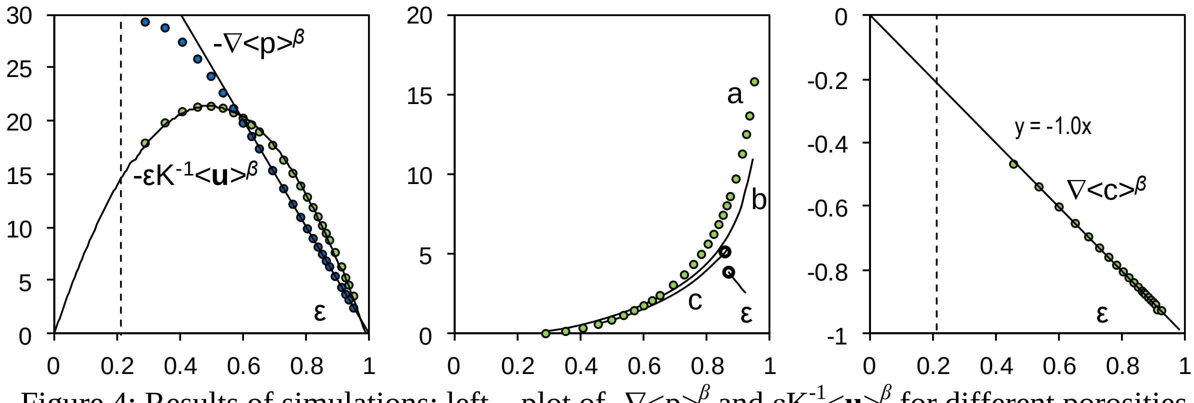

Figure 4: Results of simulations: left – plot of -∇<p>$^{\beta}$ and εK^{-1}<**u**>$^{\beta}$ for different porosities (for case 1); middle: *(a)* <**u**>$^{\beta}$ (case 1), *(b)* <**u**>$^{\beta}$ calculated from (4) (case 1), (c) plot of ε^{-1}<**u**>$^{\beta}$ (case 2); right – plot of ∇<c>$^{\beta}$ within membrane (case 2)

The calculated quantities $\tilde{\mathbf{F}} = \varepsilon K^{-1} \langle \mathbf{u} \rangle^{\beta}$ and -∇<p>$^{\beta}$ are plotted in Fig. 4 (left) with respect to the porosity ε of the membrane. While $\tilde{\mathbf{F}}$ is closely parabolic, the dependence of the averaged pressure gradient is mostly linear. Despite the difference the Darcy law (4) acceptably captures the relationship between averaged velocity and pressure (Fig. 4, middle).

In the second series of calculations (case 2) due to the decrease of the concentration gradient within the membrane the averaged velocity decreases as compared with the unperturbed case (case 1). The magnitude of the concentration gradient within the membrane in this situation is proportional to the porosity ε (Fig.4, right). Plotting the quantity $\varepsilon^{-1}\langle \mathbf{u} \rangle^{\beta}$ (Fig.4, middle), it corresponds to the magnitude of the averaged velocity $\langle \mathbf{u} \rangle^{\beta}$ in the unperturbed case (case 1). This correspondence remains up to rather large values of porosity. The little difference can be attributed to convective dispersion within the membrane.

Starting from a certain value of porosity ($\varepsilon \approx 0.85$) the dependence experiences a discontinuity and the averaged velocity begins do decrease. This happens due to the establishing of the instability of the flow. The symmetrical configuration is replaced by the asymmetrical one and further increasing the porosity ($\varepsilon > 0.95$) we observed periodic oscillations.

4. Conclusions

We have performed pore-scale numerical simulations of ferrofluid magnetosolutal microconvection in 1D ordered porous membranes composed of cylindrical elements. The imbalance of concentration was created by thermophoretic separation induced by a temperature gradient. The application of external magnetic field creates highly inhomogeneous distribution of magnetic force within the membrane, which nevertheless possesses well-defined macroscopic structure. A pressure difference appears across the membrane driving the flow of ferrofluid in the direction of the temperature gradient. We show that interpretation of the results of pore-scale simulations in the framework of the Darcy theory is possible, although errors as high as 30% can take place in some cases.

Acknowledgements

The work has been supported by the European Social Fund, Project 2013/0018/1DP/1.1.1.2.0/13/APIA/VIAA/061

5. References

[1] Blums, E.Ya.: Thermomagnetophoresis of particles in a magnetic suspension. Magnetohydrodynamics 15 (1979) 18-22.

[2] Bacri, J.C.; Cebers, A.; Bourdon, A.; Demouchy, G.; Heegaard, B.M.; Perzynski, R.: Forced Rayleigh Experiment in a Magnetic Fluid. Phys. Rev. Lett. 74 (1995) 5032-5035.

[3] Morozov, K.I.: Gradient diffusion in concentrated ferrocolloids under the influence of a magnetic field. Phys. Rev. E 53 (1996) 3841-3846

[4] Maiorov, M.M.; Tsebers, A.O.: Magnetic microconvection of the diffusion front of ferroparticles. Magnetohydrodynamics 19 (1983) 360-368.

[5] Zablotsky, D.; Mezulis, A.; Blums, E.: Formation of magnetoconvection by photoabsorptive methods in ferrofluid layers. C. R. Mecanique 341 (2013) 449-454.

[6] Blums, E.; Sints, V.; Kronkalns, G.; Mezulis, A.: Non-isothermal separation of ferrofluid particles through grids: Abnormal magnetic Soret effect. C. R. Mecanique 341 (2013) 348-355.

[7] Blums, E.; Sints, V.; Mezulis, A.; Kronkalns, G.: New problems of mass transport in magnetic fluids. Magnetohydrodynamics 49 (2013) 360-367.

[8] Blums, E.: New transport properties of ferrocolloids: magnetic Soret effect and thermomagnetoosmosis. JMMM 289 (2005) 246-249.

[9] Frishfelds, V.; Blums, E.: Drift of ferrocolloids through a cylindrical grid by magnetic force. J. Phys.: Condens. Matter 20 (2008) 204130

[10] Blums, E.; Cebers, A.; Maiorov, M.: Magnetic Fluids. Walter de Gryuter, Berlin, New York, 1997.

[11] Quintard, M.; Whitaker, S.: Transport in Ordered and Disordered Porous Media I-V. Transport in Porous Media 14 (1994), 163-206, Transport in Porous Media 15 (1994), 31-196